The effect of water absorption on the dielectric properties of epoxy nanocomposites

Chen Zou, J C Fothergill
Department of Engineering, University of Leicester, Leicester, LE1 7RH UK

and S W Rowe
Schneider Electric Industries S.A.S, Grenoble, France

ABSTRACT

In this research, the influence of water absorption on the dielectric properties of epoxy resin and epoxy micro-composites and nano-composites filled with silica has been studied. Nanocomposites were found to absorb significantly more water than unfilled epoxy. However, the microcomposite absorbed less water than unfilled epoxy: corresponding to reduced proportion of the epoxy in this composite. The glass transition temperatures of all the samples were measured by both differential scanning calorimetry and dielectric spectroscopy. The T_g decreased as the water absorption increased and, in all cases, corresponded to a drop of approximately 20K as the humidity was increased from 0% to 100%. This implied that for all the samples, the amount of water in the resin component of the composites was almost identical. It was concluded that the extra water found in the nanocomposites was located around the surface of the nanoparticles. This was confirmed by measuring the water uptake, and the swelling and density change, as a function of humidity as water was absorbed. The water shell model, originally proposed by Lewis and developed by Tanaka, has been further developed to explain low frequency dielectric spectroscopy results in which percolation of charge carriers through overlapping water shells was shown to occur. This has been discussed in terms of a percolation model. At 100% relative humidity, water is believed to surround the nanoparticles to a depth of approximately 5 monolayers. A second layer of water is proposed that is dispersed by sufficiently concentrated to be conductive; this may extend for approximately 25 nm. If all the water had existed in a single layer surrounding a nanoparticle, this layer would have been approximately 3 to 4 nm thick at 100%. This "characteristic thickness" of water surrounding a given size of nanoparticle appeared to be independent of the concentration of nanoparticles but approximately proportional to water uptake. Filler particles that have surfaces that are functionalized to be hydrophobic considerably reduce the amount of water absorbed in nanocomposites under the same conditions of humidity. Comments are made on the possible effect on electrical aging.

Index Terms — **water absorption, epoxy, nanocomposites, glass-transition temperature, differential scanning calorimetry, dielectric spectroscopy, swelling, percolation, electrical aging**

1 INTRODUCTION

EPOXY resins are highly crosslinked amorphous polymers used for the insulation of power transformers, switchgear, rotating machines, etc. The sensitivity of epoxy composites to humidity is a serious matter of concern because absorption of water may cause significant and possibly irreversible changes to the material [1][2][3].

Epoxy resins can absorb up to a few weight percent of water in a humid environment, leading to an overall degradation of the dielectric properties [3]. Such a situation might be further exacerbated by inorganic fillers, which are often used to improve their mechanical and thermal properties and to reduce their cost.

The synthesis of nanometer-sized particles is becoming routine. Because their length scale is comparable to that of polymer molecules and the high specific area of the particle surfaces within a composite, nanoparticles exhibit novel properties as fillers. Recently, research incorporating various nanoparticles into existing dielectric systems in a cost effective manner has resulted in nanocomposites with improved benefits over conventional filler systems

[4][5][6][7][8]. However, the effect of water on nanocomposites is still far from being well established. Since the epoxy – particle interface is a potential location for water [9], nanocomposites with very high specific areas may be particularly vulnerable to the effects of such water. It is possible that a weakness caused by water will have a detrimental effect on the otherwise improved mechanical [10][11] and electrical behaviors experienced by incorporating nano-fillers.

In this research, we have examined epoxy resin both unfilled and filled with nano- and micro- particles as a function of humidity. Both types of particle had "natural" surfaces – i.e. the surfaces had not been modified and were not functionalized to make them hydrophobic.

It is proposed in this paper that water may collect around such particles when such composites are subject to a humid environment. It has been known for a long time that water will displace resin from glass. For example, Kinloch, in his celebrated book [13], cites the case of glass tiles, bonded with epoxy, falling off a bathroom wall in a London hotel. This problem was subsequently remedied by the application of a silane primer, which presented a hydrophobic surface on the glass tiles. Clearly, in GRP technology, silanes are used as a matter of course, because water will displace resin from glass, there would otherwise be no fiberglass boats or warships.

In this paper, we present measurements of the dielectric spectrum, water uptake, swelling and density change, depression of glass transition temperature, and low-frequency charge transport processes to support the hypothesis that water collects around silica nano-particles whose surfaces have not been made hydrophobic. Preliminary results on epoxy nanocomposites filled with silica with hydrophobic surfaces are also reported and show different dielectric properties. Little pertinent work has been done in this area.

Zhao and Li [14] have reported the effect of water absorption on alumina filled epoxy nano-composites. They showed that the alumina nanoparticles increased the stiffness of the matrix and increased the dielectric constant. They noted that the dielectric constant increased greatly with water absorption and that mechanical properties generally declined.

Zhang *et al* [15][16] compared the dielectric properties of alumina filled epoxy and low-density polyethylene nanocomposites. In the range 10^{-2} to 10^{6} Hz, the polyethylene nanocomposites displayed significant interfacial polarization whereas this was not found in the epoxy nanocomposites.

2 EXPERIMENTAL

2.1 MATERIALS

The epoxy resin was manufactured using

- an epoxy resin (a polar low viscosity thermosetting diglycidyl ether of bisphenol A, Vantico, Araldite CY 225),
- a hardener (methyltetrahydrophtalic anhydride + flexibiliser di-ester di-acide, Vantico, HY 227), and
- a catalyst (n, n dymethylamine Ciba-Geigy DY 062).

The fillers used in the "nanodielectic" composites comprised nanoparticles of SiO_2 that were manufactured and supplied by Rensselaer Polytechnic Institute, New York with an average diameter of 50 nm. Their surface was not functionalized. The particles have been described and characterized in more detail in reference [12]. For the "microdielectric composites", particles of quartz (SiO_2) were used as a filler and had an average grain size of 60μm with a relatively wide distribution (since their diameter could be as high as 160μm). These are described in more detail in reference [18] and correspond to a composite that is used commercially. Epoxy resin composites with 3 or 9 wt% nano-silica fillers are here referred to as *n3* and *n9*. These were prepared for comparison with the epoxy resin without fillers (referred to as the epoxy matrix) and with 60 wt% micro-silica fillers, referred to as *M60*.

The stochiometries of the various components used in the epoxy resin (recommended by the manufacturers) and composites are shown in Table 1.

Table 1: Stochiometries of components used in epoxy resin and composites

Material	**Matrix**	***M60***	***n3***	***n9***
Resin				
CY 255	49.85%	19.98%	48.17%	45.33%
Hardener				
HY 227	49.85%	19.98%	48.17%	45.33%
Filler	0.00%	59.93%	3.37%	9.07%
Accelerator				
DY062	0.30%	0.12%	0.29%	0.27%
Total	**100.00%**	**100.00%**	**100.00%**	**100.00%**

Prior to mixing, the resin and hardener were placed in beakers in a vacuum oven (10^3 Pa, 333K) for approximately 2 hours to remove water and for pre-heating. The fillers were desiccated at 423K at 10^3 Pa overnight (17 hours) and then cooled to 333K. The epoxy and hardener were mixed thoroughly at 10^3 Pa, 333K for 15 minutes using a powerful mixer (500 r.p.m.). The filler was gradually mixed in using the same powerful mixer over the next 45 minutes under vacuum. Finally, the catalyst was added and stirred for a further 15 minutes. The fluid was then cast into plate moulds assisted by a vacuum pump. They were cured at 10^2 Pa, 373K for 2 hours and post-cured after removal from the mould at 403K (atmospheric pressure); weights were used to keep them flat. They were gradually cooled to 333K for 4 hours to allow residual stresses to dissipate.

The specimens were inspected by eye (for obvious defects) and then by SEM (Phillips XL30 ESEM, FEI Company, Hillsboro, Oregon, USA) to check for adequate dispersion of the particles. Figure 1a shows a typical micrograph for the *n3* system indicating good dispersion. The *n9* system was also generally well dispersed, although Figure 1b shows a region in which there is more agglomeration than usual.

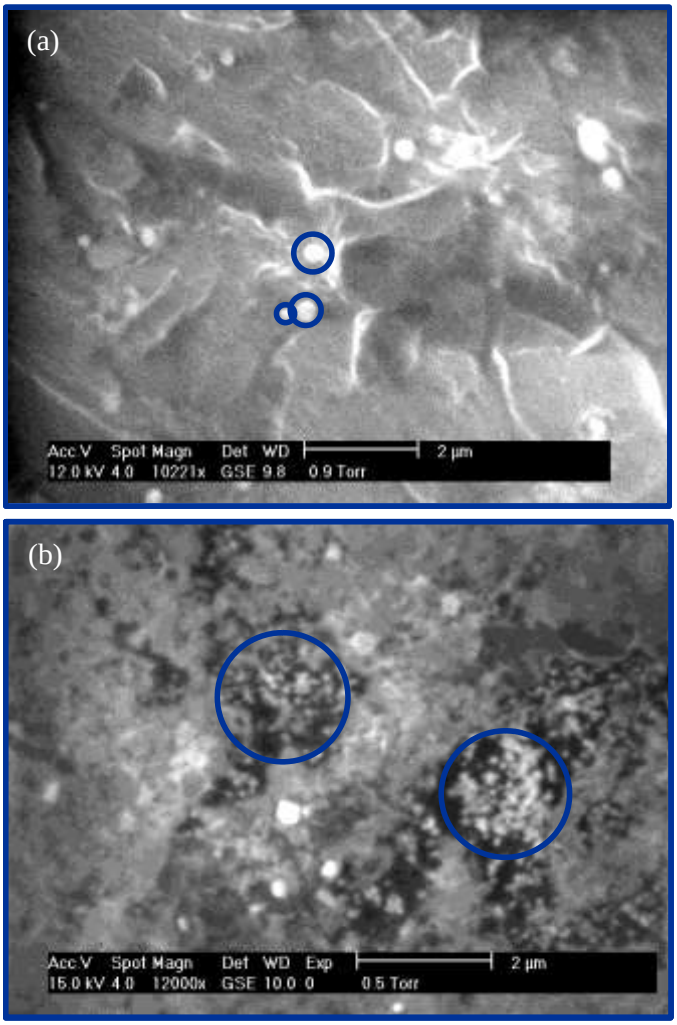

Figure 1: SEM photographs. (a) Nanocomposite *n3* with some nanoparticles circled. (b) Nanocomposite *n9* with some regions of nanoparticles circled.

All samples were cut into disks with a diameter of 60±1 mm and a thickness of 0.4±0.1 mm.

2.2 CONTROL OF RELATIVE HUMIDITY

Five conditions of relative humidity (RH %) were chosen for the testing. These were:

- Nominally 0% RH: Samples were dried in a vacuum oven (373K, 10^2 Pa) for 72 hours and subsequently kept in an atmosphere dried by silica gel to <3% RH;
- Nominally 30% RH: Samples were kept in a sealed container containing a beaker of saturated $MgCl_2$ solution resulting in an RH of 26-33% over the temperature range used of 298 to 353 K;
- Nominally 50% RH: atmosphere exposed to saturated NaBr solution, actual RH 51-59%;
- Nominally 75%RH: atmosphere exposed to saturated NaCl solution, actual RH 70 to 75%;
- Nominally 100% RH: Samples were immersed in de-ionized water at room temperature for one week and subsequently kept in atmosphere exposed to de-ionized water, resulting in 100% RH.

The method for controlling the relative humidity was obtained from references [19] and [20].

Before measurement, the samples were stored under the same humid environment as that required for at least one week to come into equilibrium (*vide infra*, Figure 2). All the samples were "stood-up" to permit water diffusion to occur from both sides of the samples during the process of water absorption. The sample weights (1.3 – 3.4 g) were monitored by a microbalance (Sartorius E400D, OHAUS Corp, USA) to an accuracy of 0.001 g to confirm that equilibrium had been reached at a given relative humidity and temperature (293K). Since the measurement uncertainty is 0.001g, this provides an accuracy of better than 0.1%.

2.3 DIELECTRIC SPECTROSCOPY MEASUREMENT

Dielectric spectroscopy is a powerful experimental method to investigate the dynamical behavior of a sample through the analysis of its frequency dependent dielectric response. This technique is based on the measurement of the complex impedance (usually expressed as capacitance when measuring dielectrics) as a function of frequency of a sample sandwiched between two electrodes.

The dielectric measurements in the frequency range 10^{-3} to 10^5 Hz were carried out by means of Solartron 1255 HF Frequency Response Analyzer, and Solartron 1296 Dielectric Interface. The temperature of the measurements was controlled in the range 298 - 353 ±0.5 K. A sealed electrode chamber was designed to maintain a constant humidity during the dielectric spectroscopy measurements. This contained a 3-electrode system (i.e. with a guard ring configuration) in which the samples were sandwiched between 50 mm diameter brass electrodes (ground flat and polished) under the force of the weight of the top electrode (1 kg). A voltage of 1 V RMS was used. This was selected after checking linearity by using measurements at 0.3 V and 3 V. The frequency was accurate to within 1 part in 10^5. The measurements of real and imaginary parts of capacitance are generally accurate to within 5%. For measurements in which the $\tan\delta<10^{-3}$, considerable noise can be present on the *C″* component.

3 RESULTS

3.1 WATER DIFFUSION IN EPOXY SAMPLES

Water diffusion in epoxy materials was measured at room temperature and nominally 75% RH, which was controlled by NaCl saturated solution (75.29 %RH at 298K, according to literature [19]). The weights of epoxy samples were monitored at different time intervals after they were put in a sealed chamber under a specific relative humidity. The samples were periodically removed from the humid environment, wiped down, and quickly weighed on the microbalance. This process was repeated until the weight did not change.

Under this experimental condition, since the relative humidity of the atmosphere is stable (~75%RH); we may expect a Fickian diffusion behavior. The mass of water absorbed, *M*, as a function of time, *t*, can be found according to equation (1) [21]:

$$M = \int_0^t J_1 dt = \sqrt{\frac{4Dt}{\pi}} BC_1 \quad (1)$$

where J_1 is the flux of moisture, B is a constant of integration; D is the water diffusion coefficient, depending on the nature of the substances, i.e., water and epoxy; t is the diffusion time of water; and C_1 is the concentration of water in the environment, i.e., 75%.

The water diffusion behavior in these epoxy samples is shown in Figure 2. Figure 2 is plotted as linear weight increase (%) versus the square root of time (hours) – so that a straight line supports equation (1).

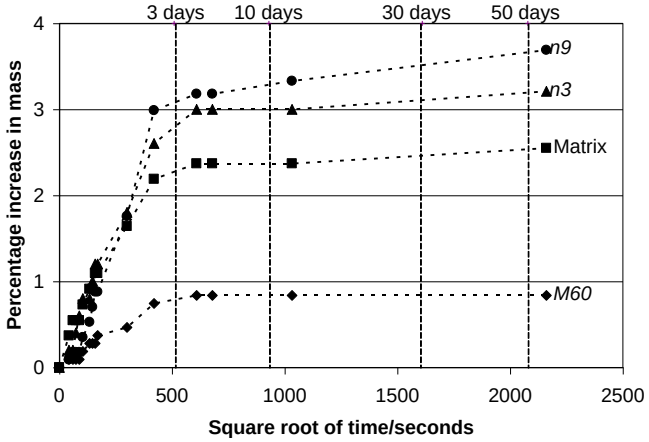

Figure 2: Water diffusion in epoxy samples (75% RH, 298K)

It is noted the % wt of water absorbed comes into quasi-equilibrium after time $t \approx 250{,}000\,\mathrm{s} \approx 3\,\mathrm{days}$ (i.e. $\sqrt{t} = 500\,\mathrm{s}^{0.5}$) in all four epoxy samples. From the initial linear portion of the curves the diffusion coefficients, *D*, for water in epoxy matrix can be calculated: *M60*, *n3* and *n9* were $3.67 \pm 1.31 \times 10^{-13}$, $0.38 \pm 0.13 \times 10^{-13}$, $5.08 \pm 1.13 \times 10^{-13}$ and $5.17 \pm 1.34 \times 10^{-13}\ \mathrm{m^2 \cdot s^{-1}}$, respectively. The diffusion coefficients of the nanocomposites are very close, whereas the *D* value for the microcomposites is lower. Diffusion through the microcomposites is severely restricted by the blocking effect of the particulate (50% by volume). The slight increases in diffusion coefficient for the nanocomposites above that of the unfilled epoxy may suggest a more continuous path for water percolation in the material.

During water diffusion, two processes may be discerned in nanocomposites. The first one is the initial linear portion of the curves in Figure 2 ($\sqrt{t} < 500\,\mathrm{s}^{0.5}$), in which water diffusion occurs and follows Fick's law. After that, another much slower process appears to occur possibly related to a gradual response of the epoxy structure to the percent of the water, and this process is described by the later flat portion of the curves in Figure 2. According to Figure 2, though *M60* has a lower diffusion coefficient than the other epoxy samples, the water absorption in *M60* reaches a true equilibrium.

3.2 Water uptake

The water, *H%*, is expressed in mass percent (wt %) with reference to dried samples, and is determined from

$$H\% = \left| \frac{M_w - M_d}{M_d} \right| \times 100\% \quad (2)$$

where: M_w, is the wet weight of water-absorbed specimen, and M_d, is the weight of dry specimen.

The increases in mass of epoxy samples at 293 K at different humidities are shown in Figure 3. In these tests, all samples were removed from the given humidity environment after two weeks ($\sqrt{t} > 1000\,\mathrm{s}^{0.5}$ for comparison with Figure 2), dried superficially, and weighed to an accuracy of 0.001g.

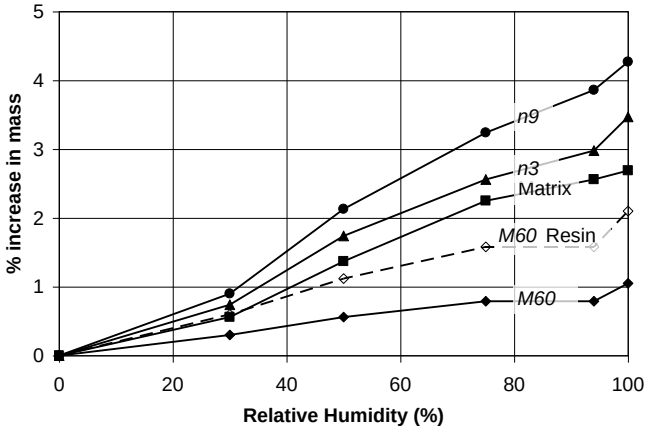

Figure 3: Water uptake for epoxy matrix and composites after two weeks at 293 K. The dotted line considers the % increase of the epoxy part (not the filler) of the *M60* composite

In all cases, the water uptake increases monotonically with relative humidity. The water uptake of the unfilled epoxy (the "matrix") increases to 2.68% at RH=100%. That of the composites filled with 60 wt% micro-particles ("*M60*") only increases to 1.3%. However, *M60* comprises 50% volume epoxy (the remainder being particles) and so it is unsurprising that the maximum uptake is approximately 50% of that of the unfilled (matrix). The curve labeled "*M60* resin" shows that the water uptake of the epoxy within the *M60* composite (i.e. ignoring the filler) and is close to that of the unfilled epoxy.

The water uptake of the 3 wt% and 9 wt% nanocomposites ("*n3*" and "*n9*") is much higher than the unfilled epoxy with the increase in water uptake of the epoxy part of *n9* being about three times that of the epoxy part of *n3*.

3.3 SWELLING AND DENSITY CHANGE

Whilst issues of swelling and cracking have been studied in epoxy resins there has been little work on epoxy nano-composites [23][24][25]. During the absorption of water, two scenarios may occur:

1. The water may occupy pre-existing space within the host material. This would be characterized by an increase in total mass with no overall volume change. Assuming that the pre-existing space was occupied by gas (e.g. atmospheric gas) this would result in an *increase in density and no swelling*. One might expect this situation to occur for an amorphous material (such as epoxy resin) where water could occupy inter-molecular spaces (possibly due to incomplete crosslinking) and small voids from deficiencies in the manufacturing. (No voids were visible. The materials were made in the same way

as other samples that were tested for partial discharge. These tests do not reveal p.d.s but there is still a possibility of the existence of small sub-micron voids.)

2. The water may force its way into the material opening up nascent cracks and structural imperfections. This would be characterized by an increase in total mass with a corresponding increase in volume. Assuming that the density of the water is less than that of the host material, this would result in *a decrease in density and concomitant swelling*. One would expect this situation to occur for composites material if it is energetically more favorable for the water to occupy sites on the surface of the particles (or the matrix) than for the matrix and particle surface to be bonded.

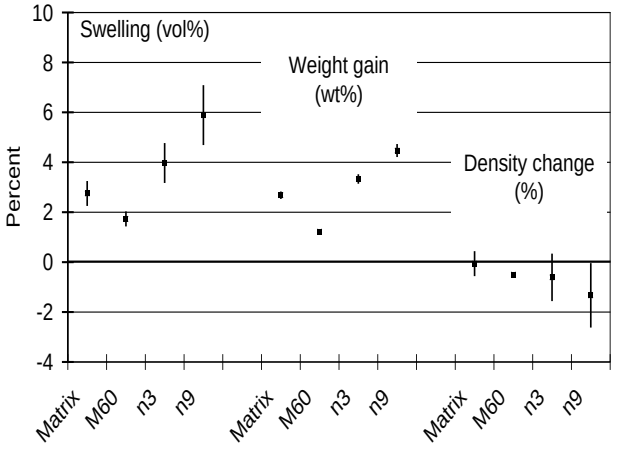

Figure 4: The swelling, weight gain and density change of water-saturated epoxy samples (bars indicate uncertainty in measurements)

Unfortunately, it was only possible to measure the dimensional change to within 1 µm (using a digital micrometer). Since the dimensional change is relatively small, the uncertainties in measurement are relatively large.

The swelling degree (vol. %), weight gain (%) and density change (%) of the samples exposed to 100% RH are shown in Figure 4.

For the matrix, there is a little swelling but little change in density. A combination of scenarios (1) and (2) may be occurring here, i.e., some filling of low-density regions within the material, but also expansion of nascent cracks. For the microcomposite, *M60*, the resultant swelling is approximately 60% (±20%) of that of the matrix, which might be explained by considering the epoxy only part of the microparticles (c.f. Figure 3). The density change is significantly less than zero, indicating a significant opening up of new surface within the composite.

In the case of the nanocomposites there appears to be considerably enhanced swelling with the 9% nanocomposites (*n9*) showing approximately three time more swelling over and above that of the matrix than that of *n3*. Similarly, the densities appear to be reduced. Under the assumption that all extra water (i.e. over and above that which would have been absorbed by the epoxy resin) evenly surrounds the nanoparticles (assumed spherical) then the thickness of the water shell around particles can be calculated, Figure 5. The dashed line in this diagram is simply a linear least squares fit. There is reasonably good agreement between the two particle concentrations (considering the difficulty in measurement) indicating an approximate shell thickness of 3 to 4 nm for 100% RH. (Since the effect of each nanoparticle is same, there must be the same amount of water around a single nanoparticle, no matter whether *n3* or *n9*.) This is also confirmed by the result that the water sorption in the epoxy part of *n9* (~4.5 vol %) is almost three times greater than that of *n3* (~1.5 vol %). This lends support to the deduction that the extra swelling in the nanocomposites is caused by incorporating the fillers around which water collects.

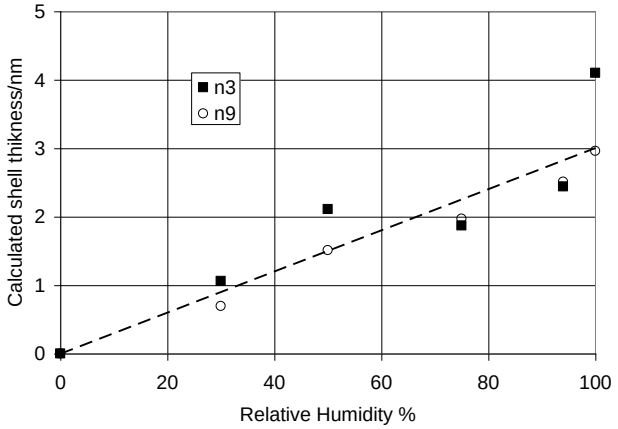

Figure 5: Calculated water shell thickness from water uptake measurements

3.4 GLASS-TRANSITION TEMPERATURE

Differential Scanning Calorimetry (DSC) measurements were used to measure the glass-transition temperature of the epoxy materials at the various relative humidities. The glass transition temperatures of all epoxy materials were tested by a modulated differential scanning calorimeter (TA Instruments, DSC 2920) with a heating/cooling rate of 10K/min from 293K to 373K and back to 293K at the same rate. The results are shown in Figure 6a.

The DSC results show that the glass-transition temperature, T_g, of epoxy samples decreases with increasing relative humidity, Figure 6a. As the environmental relative humidity increases from 0% to 100 %, the T_g of the epoxy samples decreases by ~20K. This was confirmed by dielectric spectroscopy, Figure 6b. Figure 7 shows the relation between the loss tangent and relative humidity. Using *n3* as an example, the loss tangents at 10^4 Hz were chosen to avoid the influence of relaxation peaks, since this frequency was above the relaxation process caused by water in the mid-frequency range [27].

In Figure 7, the slope of dielectric loss changes discontinuously as a function of temperature. Two linear regions can be identified in the loss tangent – relative humidity curves. The left – lower part is in the low-temperature region and so is believed to be in the glassy state. The right – upper part occurs in the high-temperature region and so is likely to be the rubbery state region. If this assumption is correct, the intersection point between the extrapolated lines can be regarded as the glass transition temperature, T_g. A similar method of determining T_g was used

by K. Fukao and Y. Miyamoto, who applied the capacitance (C') data to determine the T_g of thin films [28]. The technique has the advantage that the temperature is constant during the measurement and in therefore independent of the ramp-rate effects found using DSC. By comparing T_g at various relative humidities, it is noted that the T_g of epoxy microcomposites and nanocomposites and the epoxy matrix decreases as the relative humidity increases.

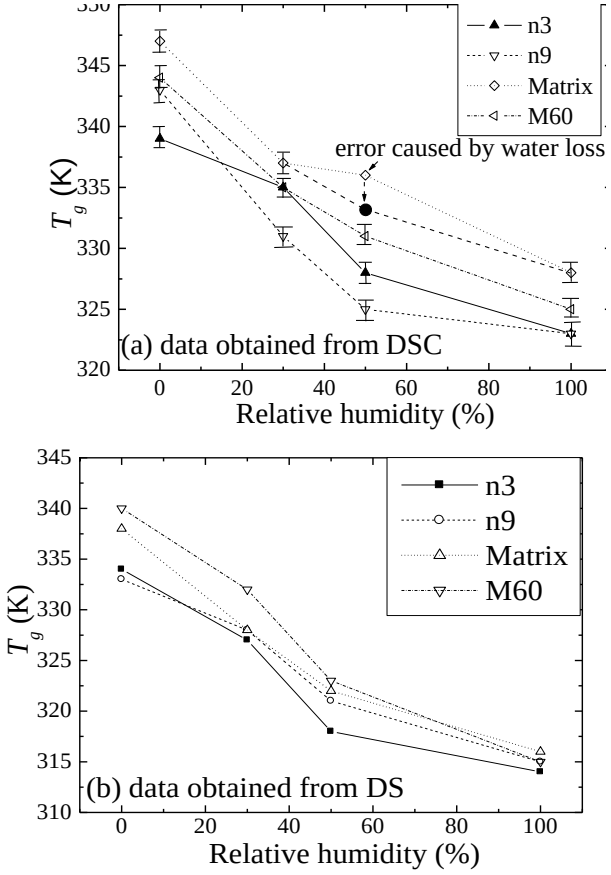

Figure 6: T_g of epoxy samples at various relative humidities. (a): measured by DSC (error ranges ±2K) and (b): measured by dielectric spectroscopy (DS) (error ranges ±2K)

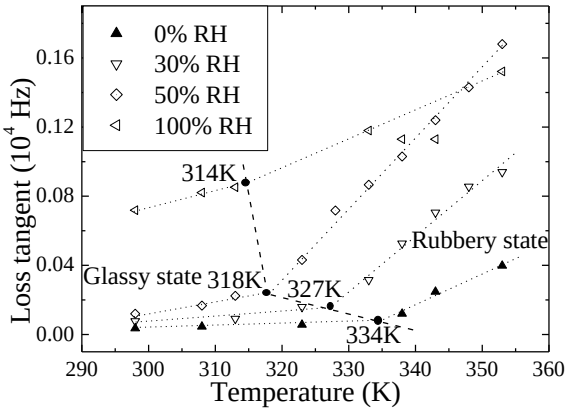

Figure 7: The variation of loss tangent of *n3* measured at 10^4 Hz as a function of temperature for different humidities indicating the glass transition temperature as a change in slope

The decrease of T_g with humidity for the unfilled epoxy resin is to be expected: an RH of 100% corresponds to approximately 2.7% wt water absorbed (293 K). Barton and Greenfield [25] showed that a decrease in T_g of approximately 10 K would be expected for every 1% wt of water absorption. In the case of the microcomposite, a similar decrease was observed: again this is to be expected since the epoxy part of this composite (dashed line in Figure 3) also absorbed about 2.7% of water at 100% RH. However, both the nanocomposites absorbed more water (3.47% and 4.27% for *n3* and *n9* respectively) and so one might have expected their T_g to have dropped further (by 6 to 12 K more). This was not observed, supporting the idea that no more water was absorbed into the epoxy resin itself and that the water therefore collected elsewhere, probably around the nanoparticles.

The effect of surfaces, such as SiO_2, on polymer dynamics is still not well understood. Kremer and Hartmann [17], for example have presented glass transition data as a function of polymer thickness (from around 10 to 10^5 nm). In some cases the T_g increases and in other cases it decreases with thickness. They conclude, "This discrepancy is presumably caused by the different surface interactions with the polymer".

3.5 THE DIELECTRIC RELAXATION PROCESS AT LOW FREQUENCIES

The dielectric spectra of the epoxy and composites were measured at various temperatures and relative humidities. The real and imaginary parts of capacitance are used to describe the dielectric behavior of composites rather than dielectric permittivity and loss as this does not require an accurate measurement of the dimensions of the sample. In Figure 8, the dielectric spectra for *n3* under conditions of RH=0% and RH=100% are presented.

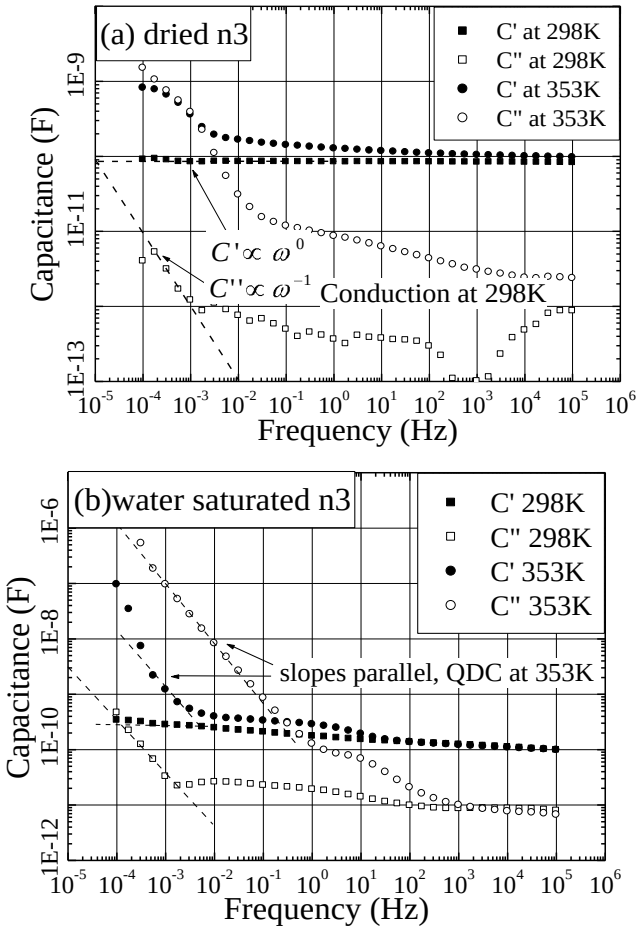

Figure 8: Dielectric spectra for *n3* at 298 K and 353 K (a) 0%, (b) 100% RH

In Figure 8a at low RH and temperature, the *n3* nanocomposite can be seen to exhibit a *C'* that is constant at low frequencies and $C'' \propto \omega^{-1}$. This is what one would expect for an ideal capacitor in parallel with an ideal conductor; i.e., it shows that there is a constant "leakage resistance" with a classical (frequency independent) conduction mechanism. For dry *n3*, the effective conductance at low frequencies at 353K is 10^{-12} to 10^{-13} S, or 10^{-14} to 10^{-15} S at 298K. However, at high RH and temperature, Figure 8b, the value of *C'* is not independent of frequency and the *C'* and *C''* curves are, in fact, parallel with a ratio *C''/C'*=73 and a slope is -0.995 in reasonable agreement with equation 4 (a slope of -0.991 would be expected) [29],

$$\frac{\chi''(\omega)}{\chi'(\omega)} \approx \cot(n\pi/2);\ 0 < n < 1 \qquad (3)$$

This was variously described as a low frequency dispersion [29] or quasi-DC (QDC) behavior [30][31][32]. This phenomenon was found in all four epoxy samples. The relative humidity and temperature of the transition from conduction to QDC is shown in Table 1. According to Table 1, with increasing concentration of nanofillers, there is a lower temperature and relative humidity environment requirement to cause to fulfill the transition from conduction to QDC.

Table 2: Low frequency dielectric behavior (conduction or Quasi-DC) under different humidities for epoxy and its composites

Samples	0% RH	30% RH	50% RH	100% RH
unfilled epoxy	Conduction	Conduction	Conduction	$\geq$ 348K QDC
M60	Conduction	Conduction	Conduction	$\geq$ 353K QDC
n3	Conduction	Conduction	Conduction	$\geq$ 343K QDC
n9	Conduction	Conduction	Conduction	$\geq$ 338K QDC

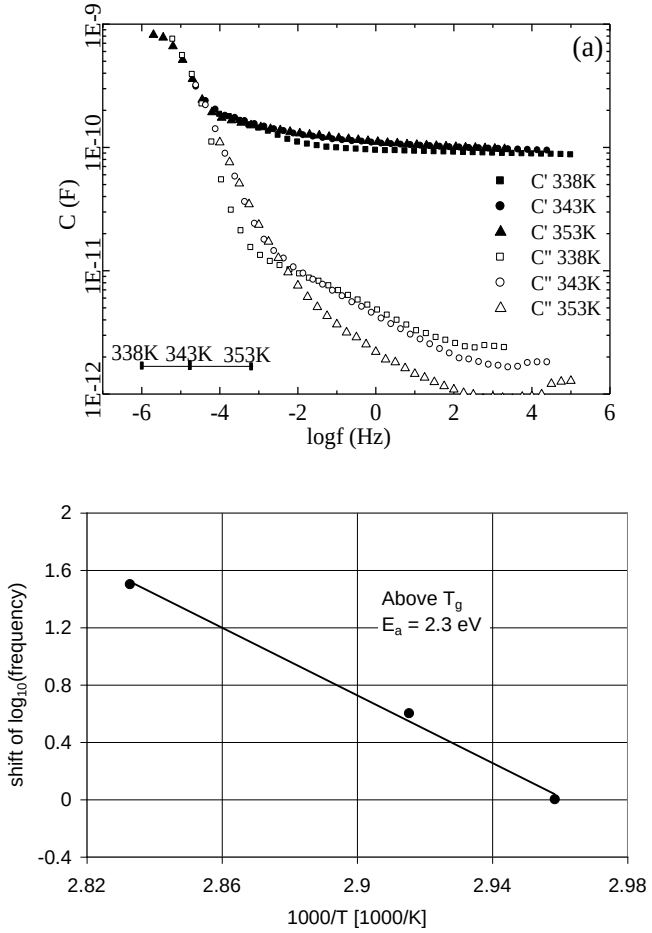

Figure 9: (a) Master plot based on low-frequency dielectric behavior for dry *n3*; (b) Arrhenius plot indicating charge transport activation energy

The time-temperature superposition assumption was made and master plots were constructed for the low frequency conduction and QDC process. An example of this is shown in Figure 9 for dry *n3*. The reference temperature in this figure is 338K. The temperature scale shows how much the plots have to be shifted to bring them into alignment at different temperatures. Such plots imply that the characteristic times governing the low frequency behavior is given by an Arrhenius-type equation

$$\tau = \tau_\infty \exp(\frac{E}{kT}) \qquad (4)$$

The activation energies for epoxy materials are shown as a function of water uptake in Figure 10.

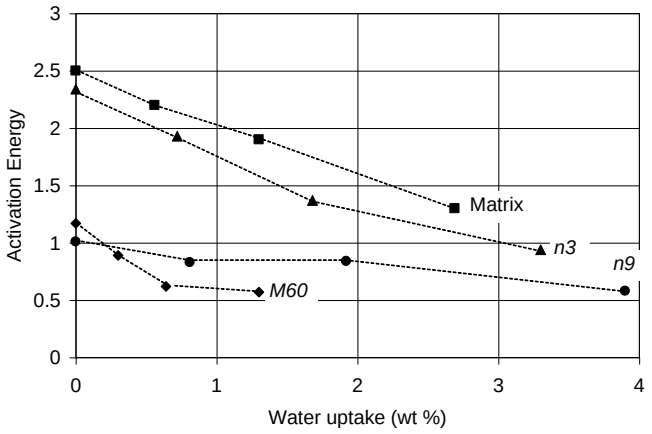

Figure 10: Low frequency charge transport activation energy of epoxy and composites for % wt of different absorbed water

The matrix and *n3* (the lesser-filled nanocomposite) behave quite similarly, suggesting that the epoxy separating the particles in *n3* is the rate-determining step for this process. As the water uptake increases, the epoxy activation energy reduces in keeping with the observation from the swelling experiment that some water is occupying low-density regions, sub-micron voids and cracks in this material. The activation energy for *n3* is, however, lower than that of the epoxy giving support to the theory that conduction is mediated around the surface of the particles. The activation energies for *n9* and *M60* (the heavily filled microcomposite) are also similar over the limited range of water uptake. It is likely that even at low water uptake, carriers can percolate through these structures. QDC (rather than pure DC conduction) is found at high humidities, where activation energies are lowest, indicates that a water-mediated percolation mechanism becomes more dominant than the DC conduction mechanism under these conditions.

4 DISCUSSION

The water absorption behavior of polymer composites in a humid environment is determined by many factors, such as processing techniques, matrix filler characteristics, composition of the composites, and so on [33]. Kinloch has studied the mechanical adhesion between epoxy and silica [10]. Without surface functionalisation treatment of the silica, Kinloch has shown that the bonding between these two materials is thermodynamically unstable in the presence of water molecules. The adhesive toughness, i.e., the energy to separate a unit area of adhesive from a substrate may become negative in the presence of water. This change from a positive to negative work of adhesion provides a driving force for the displacement of adhesive on the interface between particles and epoxy matrix by water [10] It is therefore to be expected that the interface between the inorganic fillers and matrix might be debonded by water. The higher the concentration of inorganic particles, the more debonded bonds, and the more water can be contained in this interfacial region.

When nano-particles are added to epoxy, it was found that they absorbed up to 60% more water than the unfilled epoxy or the micro-filled system, Figure 3. It is clear from these measurements that the epoxy in the micro-filled system absorbs about the same amount of water as the pure epoxy for a given humidity and that, for the micro-filled system, virtually all the water is absorbed by the epoxy. For all the systems (unfilled, micro-filled and *n3* and *n9* nano-filled), the reduction in glass transition temperature (measured by both DSC and DEA) was 20K as the samples were saturated with water. This implies that for all systems the amount of water in the resin is almost identical. The extra up to 60% of water in the nano-filled system is therefore not in the bulk resin; if it were the glass-transition temperature would be expected to drop by approximately 12K more for the saturated case. The most obvious explanation is that the extra water is located around the nano-particles forming shells in the interface zone.

4.1 WATER SHELL MODEL

According to the water uptake of the epoxy matrix and nanocomposites, the thickness of a water shell around each nanoparticle can be calculated, Figure 5 (making assumptions about the shape of the particle and shell. It is observed that the characteristic thickness of water surrounding a nanoparticle increases in rough proportion to the water uptake.

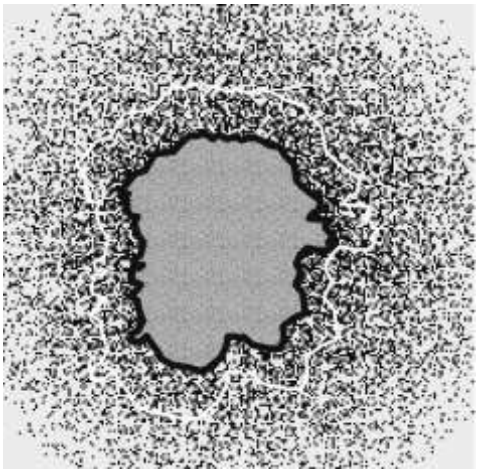

Figure 11: Schematic of a water shell surrounding a nanoparticle

Since the size of single water molecule is 0.278 nm, the thickness of a water layer is about 5-10 water molecules. This deduction is confirmed by Fourier transform infrared-multiple internal reflection (FTIR-MIR) spectra by Nguyen [34]. Bowden and Throssell found that on aluminum, iron, and SiO_2 surfaces, these layers can be up to 20 molecular layers thick at ambient temperatures and humidity [35]. To describe the real situation describing how water exists in epoxy nanocomposites, a "water shell" model is built up. In this mode [36][37], a nanoparticle plays a role of "core". To cover the "core", the water in nanocomposites can be divided into three layers. The first layer of water (~5 water molecules) may be firmly bound to the nanoparticle. Beyond that, water may be loosely bound by van der Waals Forces as the second layer. The concentration of water in this second layer may be sufficient to allow this to be conductive. The rest of the water will be "free" and exists in the bulk of the matrix. The first and second water layers are likely to provide a channel for charges and carriers. Figure 11 is an attempt to illustrate this. The nanoparticle is shown in grey in the centre surrounded by the first layer of water (shown in black). Water also surrounds

this first layer in high concentration as interconnected regions – this is the conductive layer 2 and is indicated in the figure by a white line. Outside this, the water is in a lower concentration, which may not be conductive.

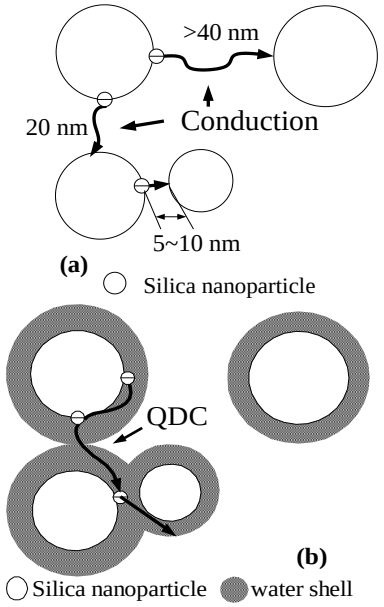

Figure 12: Charge carrier movement through overlapping water shells

For dry nanocomposites, Figure 12a, the situation in nanocomposites is that the shell will be too thin for overlap to be likely. However, once enough water enters the nanocomposites to provide the overlapping water layers surrounding nanoparticles, Figure 12b, which can provide the paths for charges and carriers, QDC behavior will occur at low frequencies. The higher content of nanoparticles, the shorter distance between particles, and less water uptake and lower temperatures are required to make the water shells around nanoparticles overlap.

4.2 PERCOLATION

For charge/carriers to percolate through overlapping shells, the volumetric concentration of zone and spherical particle must exceed 19% [38]. Figure 13 shows the required ratio of shell thickness to particle radius as a function of volumetric concentration of a spherical particle for complete percolation to occur [39]. For *n9*, the volumetric concentration is approximate 4.5%. Thus, for these 25 nm radius particles, the thickness of layers 1 and 2 must exceed 15 nm for full percolation. We would therefore expect extended charge carrier movement but at a sub-percolation level.

At low levels of RH and at lower concentration of particles, the shells would not be expected to overlap much and conduction could be largely determined by the conduction through the epoxy matrix between the particles. This would result in a low frequency dielectric characteristic in which $C' \propto \omega^0$, $C'' \propto \omega^{-1}$. This is observed in all systems at lower RH levels, table 1. In Figure 10, the higher activation energies observed at low levels of RH in the matrix are similar to that for *n3*, in which the volumetric concentration of particles is ~1.5%. In *n3*, percolation through overlapping water shell will be less common. So drift velocity for charge transport will be determined by the carrier movement through the epoxy (where it is much difficult) rather than through percolation overlapping water shell. However, in *M60* and *n9*, percolation is much more likely and the activation energy is therefore lower.

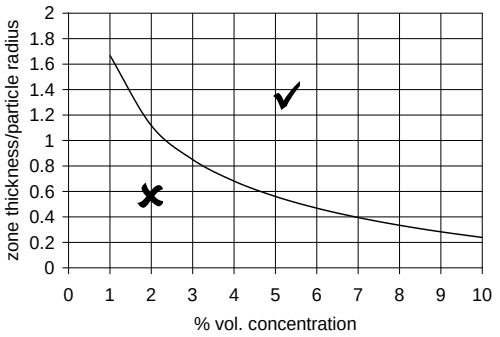

Figure 13: Percolation occurs on the "✓" side of the line (from [39]**)**

If both epoxy matrix and inorganic filler (with their interfacial phase) are considered as capacitive, it could be assumed as an elementary assumption they are in series to compose the system of epoxy composites, like that shown in Figure 14.

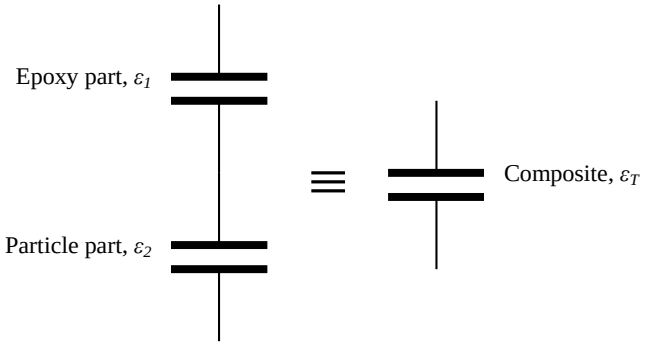

Figure 14: Consideration of particle and matrix in series

Then, the dielectric parameters of the fillers with their interfacial phase can be calculated from the results of epoxy matrix ε_1 and epoxy composites with fillers (*n3*, *n9* or *M60*), ε_T, by the equation below,

$$\frac{1}{\varepsilon_T' - i\varepsilon_T''} = \frac{p}{\varepsilon_1' - i\varepsilon_1''} + \frac{1-p}{\varepsilon_2' - i\varepsilon_2''} \quad (5)$$

where $0<p<1$ is a ratio coefficient to express the contribution that the epoxy part gives; ε_2 is the permittivity of the fillers and their interfacial phase.

Figure 15 shows, for 353K and 100% RH, calculated real and imaginary permittivities for (a) the microparticle system and (b) the *n3* nanoparticle system according to equation 5. In Figure 15a it is not possible to find a QDC behavior for any value of *p*, whereas in Figure 15b, QDC is observed for all possible values of *p*.

At high temperatures, the nanoparticles surrounded with a water shell behaved the same as the epoxy matrix, i.e., QDC at low frequencies. However, unlike nanoparticles, no matter what values of *p* were used, the dielectric relaxation of microparticles and their interface phase at low frequencies

could not be QDC. This hints that the QDC occurring in *M60* at low frequencies (under higher relative humidity and temperature) is unlikely to be due to microparticles.

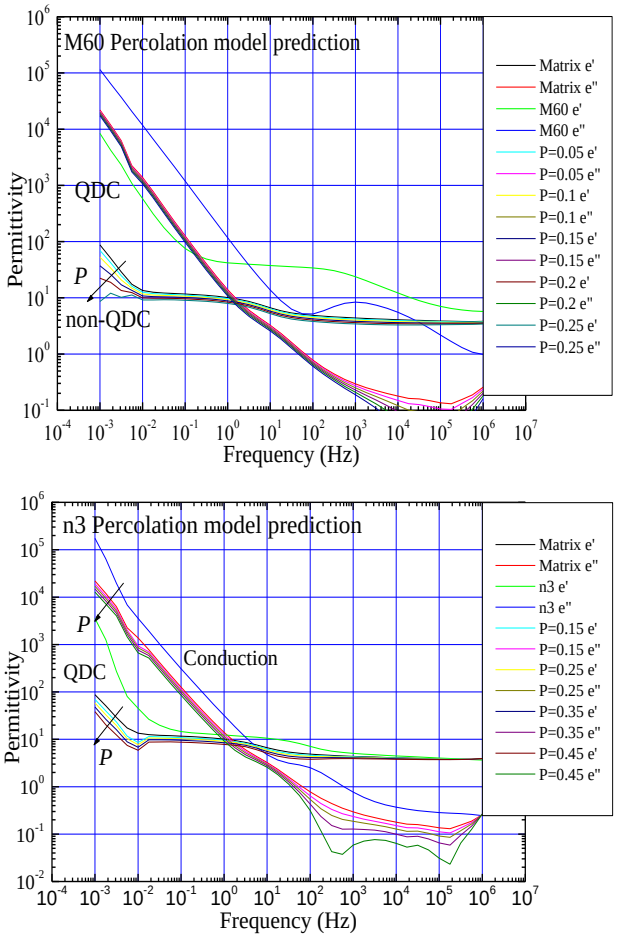

Figure 15: Calculation of complex permittivity using equation (5) for (a) micro-composite and (b) nano-composite.

4.3 SURFACE MODIFICATION

It has been pointed out that nanoparticles enhance the water absorption in nanocomposites, which is unwanted in most cases. There are two obvious solutions for this problem. One is to establish a better interfacial adhesion between the blend matrix and the particles by choosing appropriate inorganic fillers carefully. This may result in a higher density composite and a lower proportion of low-density region in the volume around the particles, so that less water can store in composites. As is well known, the higher the concentration of hydrophilic nanosilica, the more debonded bonds, and the more water can be contained in this interfacial region. Hence, the other solution is changing the surface hydrophilic into surface hydrophobic nanosilica. Since the first solution is more expensive, the second option is chosen.

Although further work is required, preliminary experiments have been carried out using a surface hydrophobic nanosilica (Degussa Gmbh, Germany). At a concentration of 3 wt% surface hydrophobic nanosilica, the water uptake of saturated epoxy nanocomposites is ~1.50%, which is much below than that of epoxy nanocomposite filled with 3 wt% normal nanosilica (~3.33%), and even less than the water uptake of the epoxy matrix (~2.48%). Surface modified nanoparticles may therefore reduce the water absorption in epoxy composites. The samples, however, were much more difficult to prepare.

4.4 AGING

Rowe [40] has proposed an "Interface degradation aging scenario" for composite materials in which the interfaces between the particles and the host material gradually weaken. In this case, the water may weaken the interface between the epoxy and silica. This accumulation of water modifies the mechanical strength, the dielectric behavior and the electrical strength of these tiny regions. Since this degradation is diffuse and occurs at all interfaces contemporaneously, it can be thought of as aging in the true sense [39]. Gradually a network of semi-interconnected pathways builds up through the labyrinth of filler particles. If percolation through these degraded regions occurs, Figure 16, then an electrical pathway forms that may lead to breakdown.

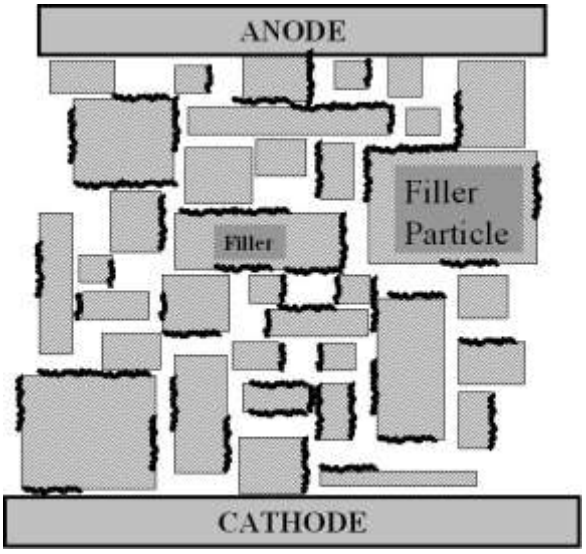

Figure 16: Interface degradation aging scenario (from [40])

This "interface degradation aging scenario" for highly filled HV insulation is fundamentally different from other explanations. In particular, the aging precursor is not dependent upon the electrical field, charge, etc. It is only after the damage has been started by the water, which is inevitably present, that electrical degradation starts to occur.

5 CONCLUSION

In this research, the effect of humidity on the dielectric properties of epoxy materials was studied. It was observed that nanofillers with unmodified surfaces enhanced the water sorption in epoxy materials, but microfillers made little contribution. The glass-transition temperature of all epoxy materials dropped by a similar amount, i.e., approximately 20K, as the relative humidity was increased from 0% to 100%. This suggested the extra water in nanocomposites did not exist in the resin component; otherwise, the T_g of nanocomposites would have an additional decrease. The results of swelling and density change between dried and water saturated epoxy materials also supported the extra water in nanocomposites

surrounds inorganic particles rather than existing in epoxy matrix. In the first stage, the diffusion of water into the samples obeys the Fick's law, but after that, the diffusion of water is controlled by another slower mechanism operative in the nanocomposites.

Under conditions of higher temperature and humidity, the dielectric relaxation process at low frequencies changes from a typical conduction current to QDC. Based on the models proposed by Lewis and developed by Tanaka, the water shell model has been further developed to explain this phenomenon in which percolation of charge carriers through overlapping water shells was shown to occur. This model is built up in terms of a percolation model. At 100% relative humidity, water is believed to surround the nanoparticles to a depth of approximately 5 monolayers. A second layer of water is proposed that is dispersed but sufficiently concentrated to be conductive; this may extend for approximately 25 nm. If all the water had existed in a single layer surrounding a nanoparticle, this layer would have been approximately 3 to 4 nm thick at 100%. This "characteristic thickness" of water surrounding a given size of nanoparticle appeared to be independent of the concentration of nanoparticles but approximately linearly dependent on water uptake.

The water uptake of nanosilica epoxy composite can be considerably reduced by ensuring that the filler particles have surfaces that are functionalized to be hydrophobic. This may also improve the composites resistance to aging.

6 ACKNOWLEDGMENT

This work is supported by EPSRC (contract number GR/530672/01), UK and Schneider Electric, France.

7 REFERENCES

[1] L.-R. Bao, F. A. Yee and C. Y.-C. Lee, “Moisture absorption and hydrothermal aging in a bismaleimide resin”, Polymer, Volume 42, Issue 17, pp. 7327-7333, August 2001.

[2] P. Bonniau and A. R. Bunsell, *J. Comp. Mater.*, 15, 272, 1981.

[3] G. Z. Xiao, M. E. R. Shanahan, “Water Absorption and Desorption in an Epoxy Resin with Degradation”, Journal of Polymer Science: Part B: Polymer Physics, Vol. 35, pp 2659–2670, 1997.

[4] J. K. Nelson, J. C. Fothergill, L. A. Dissado and W. Peasgood, “Towards an understanding of nanometric dielectrics”**,** IEEE Conf. Elec. Insulation & Dielectric Phenomena, Mexico, Oct. 2002.

[5] M. Roy, J. K. Nelson, L. S. Schadler, C. Zou, J. C. Fothergill, “The Influence of Physical and Chemical Linkage on the Properties of Nanocomposites”, Annual Report - Conference on Electrical Insulation and Dielectric Phenomena, CEIDP, pp. 183-186, 2005.

[6] C. Zou, J. C. Fothergill, M. Fu, J. K. Nelson, “Improving the dielectric properties of polymers by incorporating nano-particles”, Proc. 10th INSUCON International Electrical Insulation Conference, Birmingham, pp. 125-130, 24-26 May 2006.

[7] Nelson, J.K.; Utracki, L.A.; MacCrone, R.K.; Reed, C.W. "Role of the interface in determining the dielectric properties of nanocomposites" 2004 Annual Report conference on Electrical Insulation and Dielectric Phenomena (IEEE Cat. No.04CH37584), 2004, 314-17, ISBN-10: 0 7803 8584 5

[8] Nelson, J. K.; Hu, Y.; Thiticharoenpong, J. "Electrical Properties of TiO2 Nanocomposites" Conference on Electrical Insulation and Dielectric Phenomena (CEIDP), Annual Report, 2003, p 719-722, ISSN: 0084-9162

[9] A. J. Kinloch, M. S. G. Little, J. F. Watts, “The Role of the Interphase in the Environmental Failure of Adhesive Joints”, Acta mater. 48, pp. 4543-4553, 2000.

[10] A. J. Kinloch, Ed. *Durability of structural adhesives*” Applied Science Publishers: England, 1983.

[11] A. J. Kinloch, M. S. G. Little, J. F. Watts, “The Role of the Interphase in the Environmental Failure of Adhesive Joints”, Acta mater. 48, pp 4543-4553, 2000.

[12] Roy, M.; Nelson, J. K.; MacCrone, R.K.; Schadler, L.S. " Candidate mechanisms controlling the electrical characteristics of silica/XLPE nanodielectrics" Journal of Materials Science, v 42, n 11, June, 2007, p 3789-3799

[13] A.J. Kinloch, "Adhesion and Adhesives: Science and Technology", Chapman and Hall, 1987

[14] Hongxia Zhao and Li, R.K.Y. " Effect of water absorption on the mechanical and dielectric properties of nano-alumina filled epoxy nanocomposites" Key Engineering Materials, v 334-335, pt.1, 2007, 617-20, ISSN: 1013-9826 Publisher: Trans Tech Publications, Switzerland

[15] Zhang, C.; Mason, R.; Stevens, G. "Preparation, characterization and dielectric properties of epoxy and polyethylene nanocomposites" IEEJ Transactions on Fundamentals and Materials, v 126, n 11, 2006, p 1105-1111, ISSN: 0385-4205

[16] Zhang, C.; Mason, R.; Stevens, G.C., "Dielectric properties of alumina-polymer nanocomposites" Annual Report - Conference on Electrical Insulation and Dielectric Phenomena, CEIDP, 2005, p 721-724, ISSN: 0084-9162

[17] Kremer, F. and Hartmann, L., “Broadband Dielectric Spectroscopy and the Molecular Dynamics in Thin Polymer Layers” Dielectrics Newsletter, September 2001, pp. 4 – 6, (http://novocontrol.de/newsletter/DNL15.PDF)

[18] O Gallot-Lavallée, G Teyssèdre, C Laurent and S Rowe, "Space charge behaviour in an epoxy resin: the influence of fillers, temperature and electrode material" J. Phys. D: Appl. Phys. 38 (2005) 2017–2025

[19] “The scale of relative humidity of air certified against saturated salt solutions”, OIML R 121, Edition 1996 (E).

[20] J. Nyvlt and O. Sohnel, *Solubility in inorganic two-component systems*, Elsevier, 1981.

[21] E. L. Cussler, *Diffusion: Mass Transfer in Fluid Systems*, 2nd Edition, Cambridge University Press, 1997.

[22] S.-J. Luo, J. Leisen, C. P. Wong, “Study on Mobility of Water and Polymer Chain in epoxy and Its Influence on Adhesion”, Journal of Applied Polymer Science, Vol. 85, pp. 1-8, 2002.

[23] Liu, T.; Tjiu, W. C.; Tong, Y.; He, C.; Goh, S. S.; Chung, T.-S., " Morphology and fracture behavior of intercalated epoxy/clay nanocomposites",: Journal of Applied Polymer Science, v 94, n 3, Nov 5, 2004, p 1236-1244

[24] Ellyin, F.; Rohrbacher, C. "The influence of aqueous environment, temperature and cyclic loading on glass-fibre/epoxy composite laminates" Journal of Reinforced Plastics and Composites, v 22, n 7, 2003, p 615-636

[25] Barton, J. M.; Greenfield, D. C. L. "Use of dynamic mechanical methods to study the effect of absorbed water on temperature-dependent properties of an epoxy resin-carbon fibre composite", British Polymer Journal, v 18, n 1, Jan, 1986, p 51-56

[26] Bunsell, A.R., " Hydrothermal ageing of composite materials", Revue de l'Institut Francais du Petrole, v 50, n 1, Jan-Feb, 1995, p 61-67

[27] C. Zou, M. Fu, J. C. Fothergill and S. W. Rowe, “Influence of absorbed water on the dielectric properties and glass-transition temperature of silica-filled epoxy nanocomposites”, Annual Report - Conference on Electrical Insulation and Dielectric Phenomena (IEEE CEIDP 2006), Kansas City, MO, USA, pp 321-324, Oct 2006.

[28] K. Fukao, Y. Miyamoto, “Glass transitions and dynamics in thin polymer films: Dielectric relaxation of thin films of polystyrene”, Physical Review E, Vol. 61, No. 2, February 2000.

[29] A. K. Jonscher, *Dielectric relaxation in solids*, Chelsea Dielectric Press, ISBN:0950871109., 1983.

[30] L. A. Dissado, R. M. Hill, J. Chem. Soc., Farad. Trans., 2, **80,** pp. 291, 1984.

[31] R. M. Hill, L. A. Dissado and R. R. Nigmatullin, “Invariant behaviour classes for the response of simple fractal circuits”, J. Phys. Condens. Matter, 3, pp. 9773-9790, 1991.

[32] R. M. Hill and L. A. Dissado, “The temperature dependence of relaxation processes”, J. Phys. C: Solid State Phys., 15, pp. 5171-5193, 1982.

[33] H. V. Ramakrishna., S. K. Rai, “Effect on the mechanical properties and water absorption of granite powder composites on

toughening epoxy with unsaturated polyester and unsaturated polyester with epoxy resin", Journal of Reinforced Plastics and Composites, Vol. 25, No. 1, 2006.
[34] N. G. McCrum, B. E. Read, and G. Williams, *Anelastic and Dielectric Effects in Polymeric Solids*, Wiley, New York, 1967.
[35] F. P. Bowden, W. R. Throssell, *Nature*, *167*, 601, 1957.
[36] T. J. Lewis, 'Interfaces are the Dominant Feature of Dielectrics at the Nanometric Level', IEEE Transactions on Dielectrics and Electrical Insulation, Vol. 11, No. 5, October 2004.
[37] T. Tanaka, "Interpretation of Several Key Phenomena Peculiar to Nano Dielectrics in Terms of a Multi-Core Model", *IEEE CEIDP*, USA, 2006.
[38] X. Jing, W. Zhao and L. Lan, "The effect of particle size on electric conducting percolation threshold in polymer/conducting particle composites", Journal of Materials Science Letters, Volume 19, Number 5, pp 377-379, March, 2000.
[39] J. C. Fothergill, "Ageing, Space Charge and Nanodielectrics: Ten Things We Don't Know About Dielectrics", E O Forster Memorial Lecture, *IEEE ICSD*, Winchester, UK, July 2007 (to be published).
[40] S. W. Rowe, "Electrical Ageing of Composites: An Industrial Perspective", *IEEE ICSD*, Winchester, UK, July 2007 (to be published).

Chen Zou was born in Shaanxi, China in 1977. He received the Batchelor and Master degrees, both in electrical engineering, from Xi'an Jiaotong University, China. He completed his PhD in the Department of Engineering, University of Leicester, UK, under the sponsorship of EPSRC (UK) and Schneider Electric (France). His research area is the development and response of polymeric nanocomposite dielectric structure.

John C. Fothergill (SM'95, F'04) was born in Malta in 1953. He graduated from the University of Wales, Bangor, in 1975 with a Batchelor's degree in Electronics. He continued at the same institution, working with Pethig and Lewis, gaining a Master's degree in Electrical Materials and Devices in 1976 and doctorate in the Electronic Properties of Biopolymers in 1979. Following this he worked as a senior research engineer leading research in electrical power cables at STL, Harlow, UK. In 1984, he moved to the University of Leicester as a lecturer. He now has a personal chair in Engineering and is currently Pro-Vice-Chancellor.

Stephen Rowe (SM '98) was born in Worthing, GB, in 1952. He first worked as an apprentice in a T.V. repair shop and developed a passion for electronics. He studied electronic design at Southampton University, GB and obtained his BSc. (Hons.) specialising in electronic control systems. He then studied in France for an MSc degree, on Polypropylene Films and a doctoral thesis on EHV Capacitor insulation systems. He entered Merlin Gerin company in 1981 as head of the UHV laboratories. During the 5 years there, he undertook research work on the Electrical Breakdown of Gases. He then moved to "Volta" high current laboratory as technical manager, where he spent 3 years working with currents up to 500kA peak, (50Hz). In 1989 he moved to the Central Research Centre at Schneider Electric, Grenoble. Here he he worked, first on understanding arcing behaviour in Medium Voltage SF6 "auto-expansion" circuit breakers, then on EHV "puffer" circuit breakers, up to 400kV. In 1995, he moved to research on Vacuum circuit breakers, which he continued until 2000. His latest move was to the Materials Research Department at SE, where he presently studies solid insulation materials and in particular, electrical ageing. His objectives are the understanding of the fundamental driving forces behind long term electrical degradation of synthetic insulation materials.